THE INFRARED ABSORPTION SPECTRUM OF FLUOROFORM

by

THOMAS RICHARD REESOR

A THESIS SUBMITTED IN PARTIAL FULFILMENT OF
THE REQUIREMENTS FOR THE DEGREE OF
MASTER OF APPLIED SCIENCE
in the Department of
PHYSICS

We accept this thesis as conforming to the standard required from candidates for the degree of MASTER OF APPLIED SCIENCE

Members of the Department
of Physics

THE UNIVERSITY OF BRITISH COLUMBIA
April, 1952

ABSTRACT

The infrared absorption spectrum of fluoroform (CHF_3) has been observed in the region 400 to 5550 cm^{-1} with a Perkin-Elmer spectrometer and, in the higher regions, a multiple path absorption cell. The theoretical shapes of a parallel and a perpendicular band have been calculated and have been confirmed by the observed spectrum. The assignments of the fundamental frequencies by Rank, Schull and Pace[5] have been confirmed and the apparent discrepancy in the appearance of the 507.5 cm^{-1} band has been explained. The anharmonicity constant x_{66} has been calculated to be -0.08 cm^{-1}. All of the fundamentals except ν_2 have been remeasured to be:

ν_1 3033 cm^{-1}

ν_3 700.1

ν_4 1375

ν_5 1153

ν_6 507.5

ACKNOWLEDGEMENT

I wish to thank Dr. A. M. Crooker for his assistance and encouragement during the course of this investigation. I also greatly appreciate the assistance and co-operation of Mr. W. Ross and the technical assistance of Mr. J. Lees, Mr. A. J. Fraser and Mr. W. Maier in the Physics Shop.

I am extremely grateful for the financial assistance given by the National Research Council and the Defence Research Board.

TABLE OF CONTENTS

LIST OF FIGURES

THE INFRARED SPECTRUM OF FLUOROFORM

I INTRODUCTION

1. Previous Work

The infrared spectrum of fluoroform (CHF_3) has been observed in the region of the fundamentals by Price[1] and in the region from 4340 cm^{-1} to 14050 cm^{-1} by Bernstein and Herzberg[2]. The Raman spectrum of liquid fluoroform has been observed by Glocker and Leader[3] and Glocker and Edgell[4]. The original assignment of the fundamental vibration frequencies by Price has been changed by Rank, Schull, and Pace[5] who have made depolarization measurements in the Raman spectrum to assist in the assignment. The Raman line at 1117 cm^{-1} which is not infrared active was reassigned as ν_2 because of its intensity and polarization. Also, the original assignment by Price of ν_3 and ν_6, which he later reversed, was confirmed. The fundamental assignments of these investigators are given in Table I, page 2.

The rotational constant, B, has been measured by Bernstein and Herzberg[2] to be 0.3451 cm^{-1} and hence the moment of inertia perpendicular to the symmetry axis $I_B = 81.08 \times 10^{-40}$ g cm^2. Assuming tetrahedral angles for F-C-F ($109^\circ 28'$), the moment of inertia parallel to the symmetry axis was calculated to be $I_C = 148.7 \times 10^{-40}$ g cm^2. and the rotational constant C = 0.1887 cm^{-1}. The rotational constant B has also been measured in the microwave region by Gilliam, Edwards and Gardy[6] to be 0.34522 cm^{-1}.

Table I. Fundamental Frequencies of CHF_3

Glocker and Edgell (liquid)		Price (gas)		Rank, Schull and Pace (liquid)	
$\Delta\nu$	Assign.	Infrared	Assign.	$\Delta\nu$	Assign.
508.1	ν_{45}	509.4	ν_6 (e)	508	ν_6 CF_3(e)
696.7	ν_6	703.2	ν_3 (a)	697	ν_3 CF_3(a_1)
936.8	ν_3				
1116.5	ν_1			1117	ν_2 CF (a_1)
		1152.4	ν_5 CH(e)	1160	ν_5 CF (e)
		1209	ν_2 CF (a)		
1376.2	ν_{89}	1351.5	ν_4 CF(e)	1376	ν_4 CF (e)
3062.0	ν_7	3035.6	ν_1 CH(a)	3062	ν_1 CH (a_1)

2. Object and Scope of Present Research

An examination of Table I shows that there is still much discrepancy between the infrared and Raman data. The most notable differences are the non-appearance of the fundamental ν_2 in the infrared and the large wave number difference between the Raman and infrared values for ν_1 and ν_4. The purpose of the present research is to remeasure the fundamental frequencies and to observe whether or not the spectrum in the region from 400 cm^{-1} to 5500 cm^{-1} is compatible with the new assignment of ν_2.

II THEORY - The Symmetric Top Molecule with Special Reference to CHF_3

The CHF_3 molecule (Fig. 1) belongs to that class of molecules which has a 3-fold axis of symmetry and has two moments of inertia perpendicular to the symmetry axis equal. The molecule is thus placed in point group C_{3v} with three planes of symmetry and one symmetry axis.

1. Rotational Levels and Rotation Spectra.

Classically, the motion of the symmetric top molecule can be visualized as a rotation of the molecule about the symmetry axis which in turn precesses about another axis pointing in the direction of $\vec{P}$, the total angular momentum. The precessional frequency is $|\vec{P}|/2\pi I_B$ and the frequency of rotation about the figure axis is $\frac{1}{2\pi}\left(\frac{1}{I_C} - \frac{1}{I_B}\right)P_Z$; where I_B and I_C are the moments of inertia perpendicular to and about the symmetry axis respectively, and P_Z is the component of $\vec{P}$ in the direction of the symmetry axis. In the quantum mechanical treatment of rotation, the $\vec{P}$ corresponds to J and the P_Z corresponds to K. Thus it is intuitively obvious that $K \leq J$.

a. Rotational Energy Levels

The rotational term values of the symmetric top molecule are given by

---

The theory of the symmetric top molecule has been covered quite adequately by Herzberg.[7] Only references that have not been summarized by him will be referred to in this section.

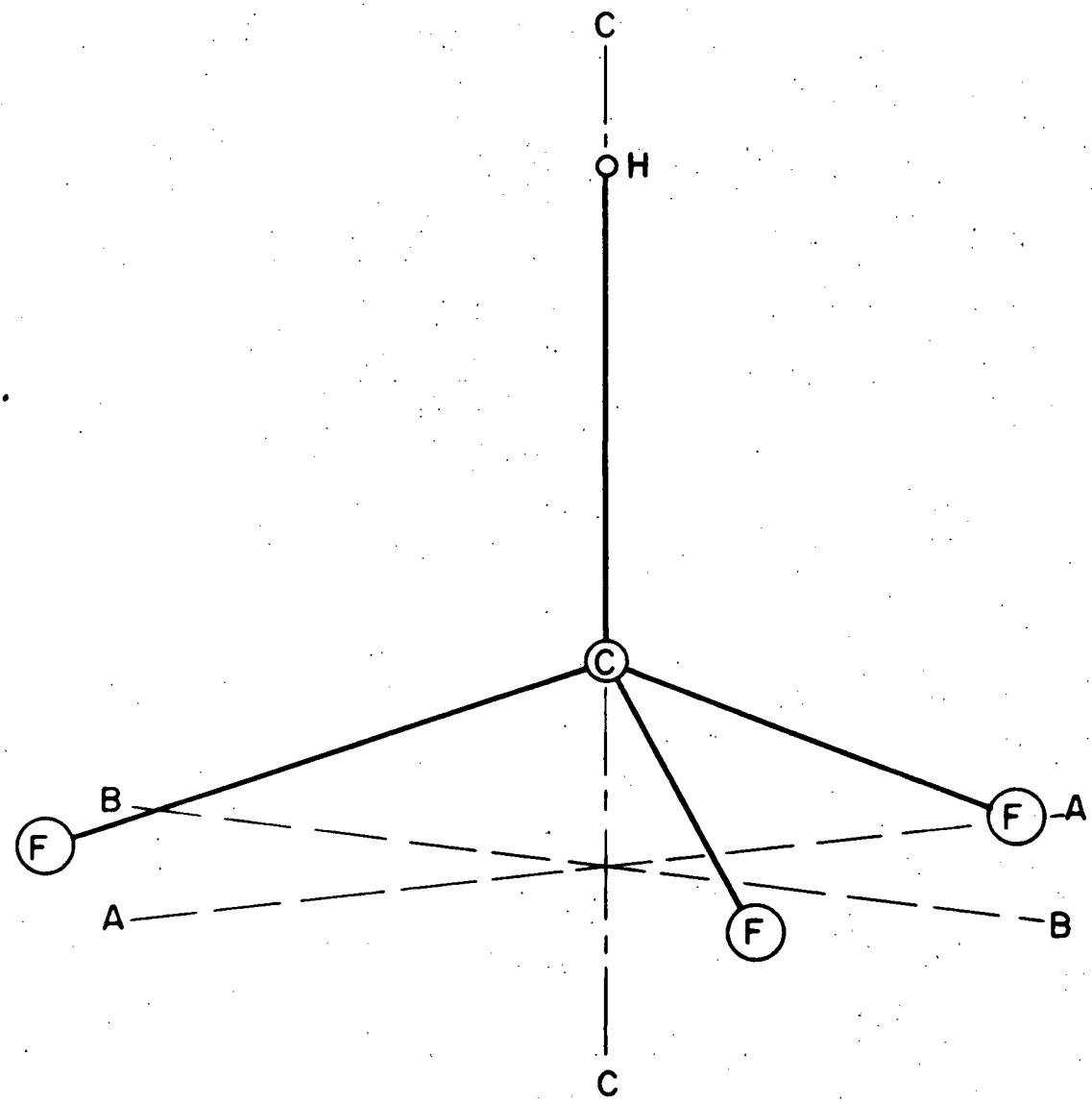

FIGURE I. THE CHF_3 MOLECULE.

$$F(J,K) = B\,J\,(J+1) + (C-B)K^2 - D_J J^2 (J^2+1)^2 - D_{JK}\,J\,(J+1)\,K^2 - D_K\,K^4$$

$K = 0, 1, 2, \ldots \qquad J = K, K+1, K+2, \ldots \qquad \ldots (1)$

where $B = h/8\pi c^2 I_B$, $C = h/8\pi c^2 I_C$ and the constants D_J, D_{JK}, and D_K are due to centrifugal stretching of the molecule due to the rotation. In most cases, except for very high resolution, only the first two terms need be considered.

Rotation levels have either positive or negative symmetry depending on whether the eigenfunction describing the state is unchanged or changes sign when all the atoms are reflected at the origin. The eigenfunctions are given by

$$\psi_r = \theta_{JKM}(\vartheta)\; e^{iK\varphi}\; e^{iM\chi} \qquad \ldots (2)$$

where ϑ , φ and χ are the Eulerian angles, M is the magnetic quantum number corresponding to the different orientations of J in space, and $\theta_{JKM}(\vartheta)$ is a complicated function of ϑ. The two modifications, positive and negative, can be transformed one to the other by passing through a potential hill. If the potential hill is not infinitely high, the two configurations will have slightly different energies causing a slight splitting of the lines (inversion doubling). In most cases this splitting requires very high resolution to measure and will be neglected in further discussion. Apart from the inversion doubling, the statistical weight or degeneracy of each level is $2J + 1$ for $K = 0$ and $2(2J + 1)$ for $K \neq 0$. In addition, there is a statistical weight due to the spin of the

identical nuclei. For a molecule of point group C_{3v}, the statistical weights are given by:

For K divisible by 3 (including zero)

$$1/3(2I + 1)(4I^2 + 4I + 3)$$

For K not divisible by 3 ... (3)

$$1/3(2I + 1)(4I^2 + 4I)$$

where I is the spin of the three identical nuclei. Thus the levels will have an intensity alteration of strong, weak, weak, strong, weak, ... where the ratio of strong to weak is $1 + 3/4I(I+1)$ :: 1 or 2:1 for CHF_3.

The population N_{JK} of the various levels is dependent on both the statistical weight and the Boltzmann distribution factor

$$N_{JK} \sim g_{JK} \; e^{-E(J,K)/kT} \qquad \ldots (4)$$

where g_{JK} is the statistical weight.

b. Rotation Spectra

An infrared rotation spectrum can appear only if the molecule has a permanent dipole moment. For a molecule of point group C_{3v}, the dipole moment will lie along the symmetry axis and the selection rules for J and K will be

$$\Delta K = 0 \qquad \Delta J = 0, \pm 1 \qquad \ldots (5)$$

In addition, the symmetry rules will be

$$+ \longleftrightarrow - \;, \quad + \not\longleftrightarrow + \quad - \not\longleftrightarrow - \qquad \ldots (6)$$

The symmetry rule will always be fulfilled for non-planar molecules since the + and - levels always occur in pairs (inversion doubling). Neglecting centrifugal stretching,

the infrared absorption lines will be given by

$$\nu = F[(J+1), K] - F[J, K] = 2B(J+1) \qquad \ldots (7)$$

The intensity of a line is given by the product of the transition probability and the population of the initial state

$$I(J,K) = C\nu \frac{(J+1)^2 - K^2}{(J+1)(2J+1)} g_{JK} e^{-F(J,K)/kT} \qquad \ldots (8)$$

where C is a constant depending on the permanent dipole moment. The intensities of the pure rotation lines will have the same distribution as in the R branch of a parallel band shown in Figure 3.

2. Vibrational Energy Levels and Vibrational Spectra

a. Vibrational Energy Levels

The natural vibration frequencies of a molecule can, in principle, be determined from classical mechanics if the force constants of the molecule are known. These frequencies will be determined by the solution of the secular equation

$$\begin{vmatrix} k''_{xx} - m_1\lambda & k''_{xy} & k''_{xz} & k'^{12}_{xx} & \cdots & k'^{1N}_{xz} \\ k''_{yx} & k''_{yy} - m_1\lambda & k''_{yz} & k'^{12}_{yx} & \cdots & k'^{1N}_{yz} \\ k''_{zx} & k''_{zy} & k''_{zz} - m_1\lambda & k'^{12}_{zx} & \cdots & k'^{1N}_{zz} \\ k'^{21}_{xx} & k'^{21}_{xy} & k'^{12}_{xz} & k'^{22}_{xx} - m_2\lambda & \cdots & k'^{2N}_{xz} \\ \cdots & \cdots & \cdots & \cdots & \cdots & \cdots \\ k'^{N1}_{zx} & k'^{N1}_{zy} & k'^{N1}_{zz} & k'^{N2}_{zx} & \cdots & k'^{NN}_{zz} - m_N\lambda \end{vmatrix} = 0 \qquad \ldots (9)$$

where k'^{ij}_{rs} is the restoring force on the i^{th} particle in the r direction due to a unit displacement of the j^{th} particle in the s direction, and $\lambda = 4\pi^2\nu^2$ where ν is the natural frequency of vibration. This equation will have 3N roots

giving rise to 3N - 6 normal vibration frequencies, where N is the number of atoms in the molecule.

The quantum mechanical treatment shows that the molecule can exist only in states that are sums of half-integer multiples of these fundamental frequencies. The Schroedinger equation of a system of N particles of masses m_i is, in Cartesian coordinates,

$$\sum_i \frac{1}{m_i}\left(\frac{\partial^2\psi}{\partial x_i^2} + \frac{\partial^2\psi}{\partial y_i^2} + \frac{\partial^2\psi}{\partial z_i^2}\right) + \frac{8\pi^2}{h^2}(E - V)\psi = 0 \qquad \ldots (10)$$

This can be reduced (Pauling and Wilson[8]) to the 3N separate equations

$$\frac{1}{\psi_i}\frac{d^2\psi_i}{d\xi_i^2} + \frac{8\pi^2}{h^2}\left(E_i - \tfrac{1}{2}\lambda_i \xi_i^2\right) = 0 \qquad \ldots (11)$$

where the λ_i[#] are the roots of the secular equation (9), $E = E_1 + E_2 + \ldots + E_i + \ldots + E_{3N}$, and the ξ_i are the normal coordinates. The eigenfunctions of equation (11) are

$$\psi_i(\xi_i) = N_{v_i}\, e^{-\frac{\nu_i \pi}{h}\xi_i^2}\, H_{v_i}\left(\sqrt{\frac{2\nu_i\pi}{h_i}}\,\xi_i\right) \qquad \ldots (12)$$

where N_{v_i} is a normalization constant and $H_{v_i}(\ )$ is a Hermite polynomial of the v_i^{th} degree. The eigenvalues of equation (11) are given by

$$E_i = h\nu_i\left(v_i + \tfrac{1}{2}\right) \qquad v_i = 0, 1, 2, \cdots \qquad \ldots (13)$$

where ν_i is the frequency of the normal vibration i and v_i is the vibrational quantum number. The total energy of the system is

---

The 3N roots will include the six non-genuine vibrations which correspond to rotation and translation and do not contribute to the vibrational energy.

$$E(v_1, v_2, \cdots) = h\nu_1 (v_1 + \tfrac{1}{2}) + h\nu_2 (v_2 + \tfrac{1}{2}) + \cdots \quad \cdots (14)$$

giving the term values (in cm^{-1} units)

$$G(v_1, v_2, \cdots) = \frac{E(v_1, v_2, \cdots)}{hc} = \omega_1 (v_1 + \tfrac{1}{2}) + \omega_2 (v_2 + \tfrac{1}{2}) + \cdots \quad \cdots (15)$$

where the $\omega_i = \frac{\nu_i}{c}$ are the classical vibration frequencies in cm^{-1}. If some of the levels are degenerate, then the term values will be given by

$$G(v_1, v_2, \cdots) = \sum_i \omega_i \left(v_i + \frac{d_i}{2}\right) \quad \cdots (16)$$

where d_i is the degree of degeneracy of the i^{th} vibration.

If the vibrations are anharmonic, which is always the case to some extent, the term values will be given by (to second order)

$$G(v_1, v_2, \cdots) = \sum_i \omega_i \left(v_i + \frac{d_i}{2}\right) + \sum_i \sum_{k \geq i} x_{ik} \left(v_i + \frac{d_i}{2}\right)\left(v_k + \frac{d_k}{2}\right) + \sum_i \sum_{k \geq i} g_{ik} l_i l_k \quad \cdots (17)$$

where d_1, is the degree of degeneracy, l_i is a quantum number of degenerate vibrations which assumes the values $v_i, v_i - 2, \cdots 1$ or 0, ω_i is the vibrational frequency for infinitesimal amplitudes, and x_{ik} and g_{ik} are anharmonicity constants.

For a molecule of point group C_{3v}, a vibrational state must be either symmetric (A) or degenerate (E) with respect to the symmetry axis, and symmetric (A_1) or anti-symmetric (A_2) with respect to the planes of symmetry. For the fundamental vibrations of CHF_3, there are three degenerate vibrations of species E and three non-degenerate totally symmetric vibrations of species A_1. The selection rules of the transition in absorption spectra depend on the species (A or E) of the initial and final states.

The species of overtone and combination states can be determined from the following rules:

$$a_1 \times a_1 = A_1 \qquad a_1 \times a_2 = A_2 \qquad a_1 \times e = E$$

$$e \times e = A_1 + A_2 + E \qquad (e)^2 = A_1 + E \qquad (e)^3 = A_1 + A_2 + E$$

$$(e)^4 = A_1 + E + E \qquad \ldots (18)$$

b. Vibrational Spectra

Normal vibrations that are accompanied by a change in the dipole moment give rise to absorption lines in the infrared and are called infrared active. All of the fundamental vibrations should be both infrared and Raman active although interaction of rotational and vibrational energy may prevent this.

The observed frequencies of the infrared absorption lines will be given by

$$G_0(v_1, v_2, \cdots) = G(v_1, v_2, \cdots) - G(0, 0, \cdots) = \sum_i \omega_i^\circ v_i + \sum_i \sum_{\kappa \geq i} x_{i\kappa} v_i v_\kappa + \sum_i \sum_{\kappa \geq i} g_{i\kappa} l_i l_\kappa \qquad \ldots (19)$$

where $\omega_i^\circ = \omega_i + x_{ii} d_i + \frac{1}{2} \sum_{\kappa \neq i} x_{i\kappa} d_\kappa$

From this, it will be noted that the observed frequency of the fundamental lines will be given by

$$\nu_{if} = \omega_i^\circ + x_{ii} + g_{ii} \qquad \ldots (20)$$

and the v_i^{th} overtone

$$(\nu_{if})^{v_i} = (\nu_{if}) v_i + v_i (v_i - 1) x_{ii} + l_i (l_i - 1) g_{ii} \qquad \ldots (21)$$

where ν_{if} and $(\nu_{if})^{v_i}$ are the actual observed transition frequencies of the fundamental and the v_i^{th} overtone respectively. It can be seen from equation (21) that the higher overtones of the degenerate vibrations will be split because the degenerate quantum numbers l_i can take all the values $v_i, v_i - 2, \ldots 1$ or 0.

Since the x_{ik} and g_{ik} are usually negative, the overtone lines will tend to converge. The observed combination line frequencies will also in general be less than the sums of the observed fundamental frequencies. The observed frequency of the difference lines, for example $\nu_1 - \nu_3$, will be exactly the wave number difference of the observed lines ν_1 and ν_3 even when anharmonicity is taken into account.

The intensities of the absorption lines are, as before, given by the product of the transition probability and the population of the initial level. As a result of this, it can be seen that the difference line $\nu_i - \nu_k$ will have a smaller intensity than the summation line $\nu_i + \nu_k$ by a factor of $e^{-\frac{\nu_k hc}{kT}}$ due to the smaller initial population in the case of the difference line. The overtone and combination lines will have a lower intensity due to a lower transition probability.

The numbering of the fundamental absorption lines of a molecule is according to the species of the vibration causing the absorption and the frequency. The largest totally symmetric frequency (species A_1 in CHF_3) is called ν_1, the second largest ν_2, and so on up to ν_f. The line with the largest frequency in the next species (the degenerate species E in CHF_3) is called ν_{f+1} and so on until all the fundamentals are labelled. Figure 2 shows the three totally symmetric vibrations ν_1, ν_2 and ν_3, and one

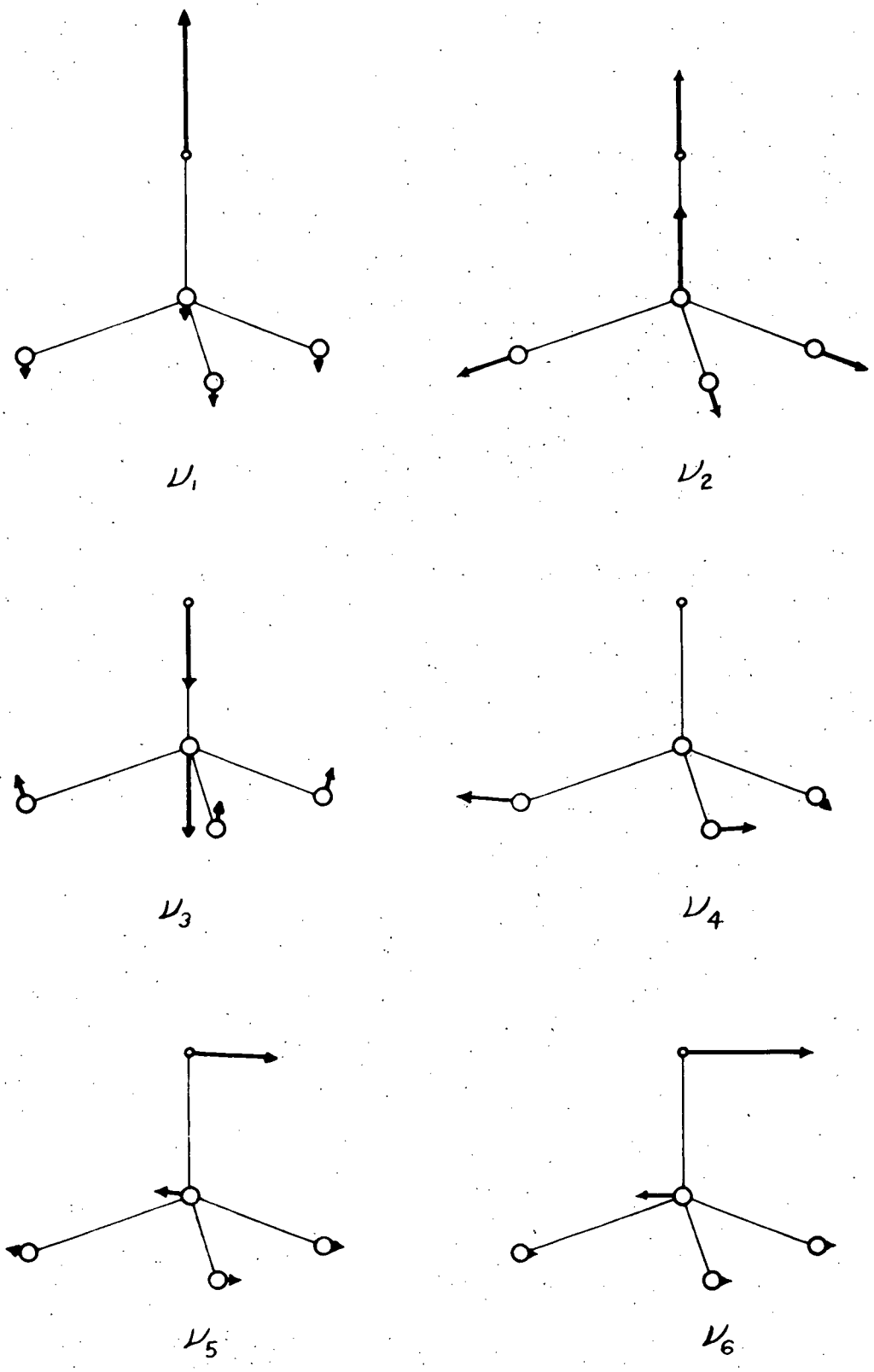

FIGURE 2. THE FUNDAMENTAL VIBRATIONS OF CHF_3

component of each of the three degenerate vibrations ν_4, ν_5 and ν_6 for CHF_3.

3. Interaction of Rotation and Vibration

a. Energy Levels

The total vibrational and rotational energy of a symmetric top molecule is given by

$$T = G(\nu_1, \nu_2, \cdots) + F_\nu(J,K) \quad \ldots (22)$$

where $$F_\nu(J,K) = B_\nu J(J+1) + (C_\nu - B_\nu)K^2 \quad \ldots (23)$$

neglecting centrifugal distortion terms. The rotational constants C_ν and B_ν are slightly dependent on the vibrational level because of the larger average dimensions of the molecule in highly excited states. To a first approximation

$$B_\nu = B_e - \sum \alpha_i \left(\nu_i + \frac{d_i}{2}\right) \quad \ldots (24)$$

where B_e is the rotational constant for zero excitation and α_i is small compared to B_e. For degenerate vibrations, the Coriolis interaction causes a splitting of the level so that the term

$$\pm 2 C_\nu \zeta_i K \quad \ldots (25)$$

must be added to the right side of equation (23). The factor ζ_i can vary from -1 to +1 and can only be calculated if the force constants of the molecule are known. If anharmonicity is neglected, the following rule holds for any XYZ_3 molecule:

$$\zeta_4 + \zeta_5 + \zeta_6 = \frac{B}{2C} \; (\simeq 0.9 \text{ for } CHF_3) \quad \ldots (26)$$

where ζ_4, ζ_5 and ζ_6 are the Coriolis constants for the singly excited vibrations ν_4, ν_5 and ν_6 respectively.

b. Infrared Spectra

Pure rotation spectra are not usually observed in infrared spectroscopy because of the long wavelengths involved. The rotational energy is usually manifested as fine structure in the vibration bands. In the case of CHF_3, the fine structure distinguishes between two distinct types of absorption bands. A parallel type of band occurs when the change of dipole moment during the transition is in the direction of the symmetry axis. The selection rules for the rotational quantum numbers for a transition that gives rise to a parallel band are:

$$\Delta K = 0, \quad \Delta J = 0, \pm 1 \text{ if } K \neq 0$$
$$\Delta K = 0, \quad \Delta J = \pm 1 \quad \text{if } K = 0 \qquad \ldots (27)$$

A perpendicular band occurs when the change of dipole moment is in a direction perpendicular to the symmetry axis. The selection rules will then be:

$$\Delta K = \pm 1 \qquad \Delta J = 0, \pm 1 \qquad \ldots (28)$$

The symmetry selection rules will always be fulfilled provided the inversion doubling is not resolved.

The detailed structure of the bands can be calculated by considering the allowed transitions and the theoretical intensities of the individual lines. Considering first the transitions between non-degenerate (A_1) levels, that is the parallel bands, it can be seen that for each value of the quantum number K there is a complete sub-band with a P brandh ($\Delta J = -1$), a Q branch ($\Delta J = 0$)and an R branch ($\Delta J = +1$). These sub-bands have origins at

$$\nu_{sub} = \nu_0 + [(C'_{\nu} - C''_{\nu}) - (B'_{\nu} - B''_{\nu})]K^2 \qquad \ldots (29)$$

where ν_0 is the frequency of the vibrational transition, C'_{ν} refers to the upper state and C''_{ν} refers to the lower state. The rotation lines will then follow the formula

$$\begin{aligned} &(\Delta J = +1)\ \text{R branch} \quad \nu = \nu_{sub} + 2B(J+1) \\ &(\Delta J = 0)\ \ \text{Q branch} \quad \nu = \nu_{sub} + (B'_{\nu} - B''_{\nu})J(J+1) \\ &(\Delta J = -1)\ \text{P branch} \quad \nu = \nu_{sub} - 2BJ \end{aligned} \qquad \ldots (30)$$

with the added restriction that $J \geqslant K$. The variation of B has been neglected in the P and R branch formulae of equation (30) because it makes no significant difference in the appearance of the band. The intensities of the lines will be given by the Hönl London formulae

$$I = C\, A_{JK}\, \nu\, g_{JK}\, e^{-F(J,K)\frac{hc}{kT}} \qquad \ldots (31)$$

where C is a constant depending on the vibrational transition, g_{JK} is the statistical weight including the rotational level degeneracy of $2J + 1$ for $K = 0$ and $2(2J + 1)$ for $K \neq 0$, and the nuclear spin intensity ratio given by equation (3). The factor A_{JK} is given by

$$\begin{aligned} \Delta J = +1 \qquad & A_{JK} = \frac{(J+1)^2 - K^2}{(J+1)(2J+1)} \\ \Delta J = 0 \qquad & A_{JK} = \frac{K^2}{J(J+1)} \\ \Delta J = -1 \qquad & A_{jk} = \frac{J^2 - K^2}{J(2J+1)} \end{aligned} \qquad \ldots (32)$$

where J and K refer to the initial state in all of the above formulae.

The detailed structure of a parallel band has been calculated for CHF_3 on the basis of these formulae and is shown in Figure 3. The values $C = 0.189\ cm^{-1}$, $B = 0.345\ cm^{-1}$ and $[(C'_{\nu} - C''_{\nu}) - (B'_{\nu} - B''_{\nu})] = .001\ cm^{-1}$

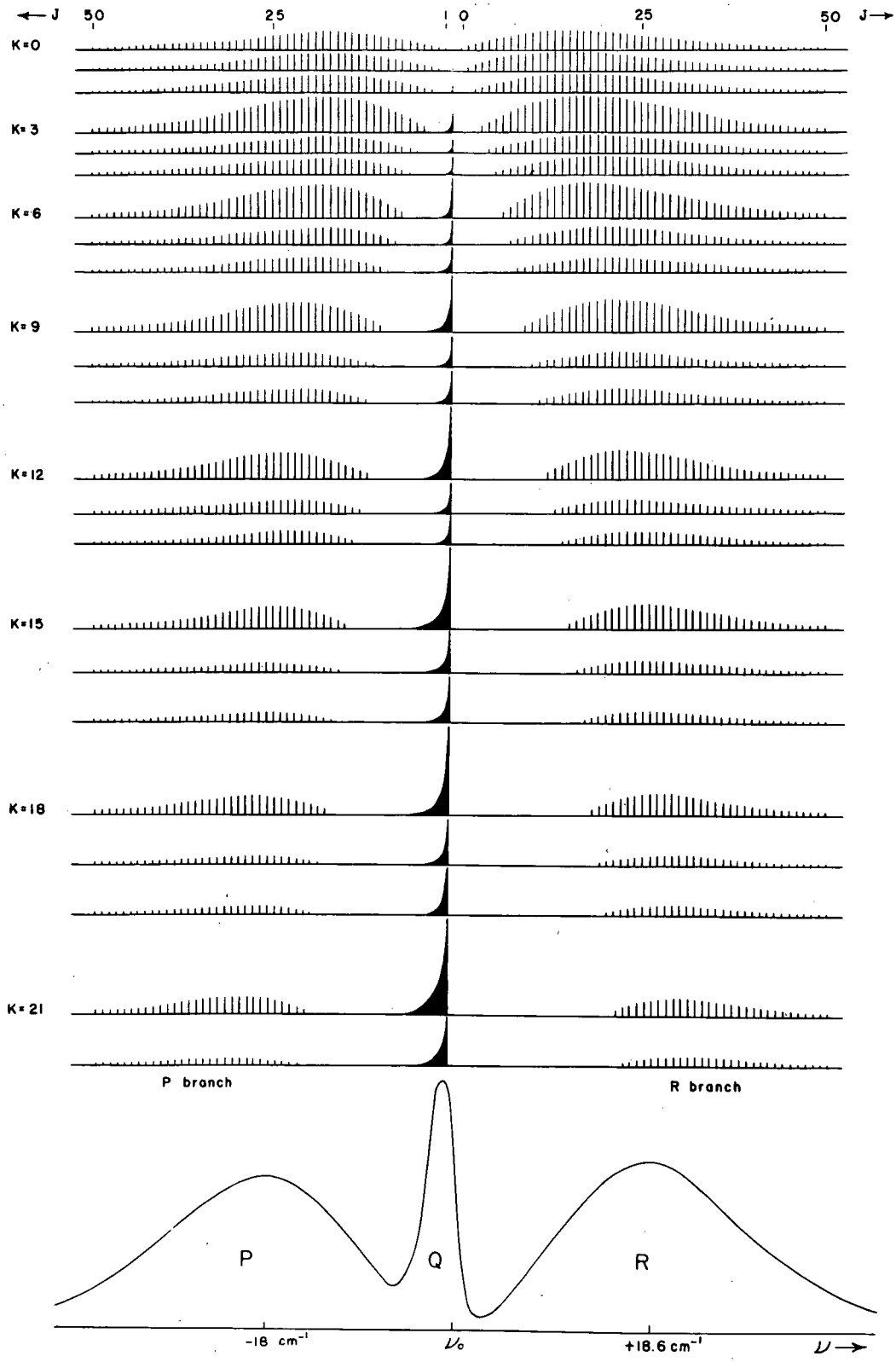

FIGURE 3. SUB-BANDS AND COMPLETE PARALLEL BAND OF CHF_3.

The intensity of the Q branches increases up to K=24 and then decreases. Total Q branch intensity should be greater than indicated. T=300°K.

were used in these calculations. The separation between the envelope peaks of the P and R branches is 37 cm^{-1} in contrast to Gerhard and Dennison's[9] value of 33 cm^{-1} calculated from the formula#

$$\Delta\nu = \frac{S(\beta)}{\pi c}\sqrt{\frac{kT}{I_B}} \qquad \ldots (33)$$

where $\log_{10} S(\beta) = \frac{0.721}{(\beta+4)^{1.13}}$ and $\beta = \frac{C}{B} - 1$

Transitions between a non-degenerate (A) and a degenerate level(E) give rise to perpendicular type bands. This condition applies to the fundamentals of the degenerate vibrations. The origins of the sub-bands for each value of K are given by:

$$\nu_{sub} = \nu_0 + [(C'_\nu)(1-2\zeta_i) - B'_\nu] \pm 2[C'_\nu(1-\zeta_i) - B'_\nu]K + [(C'_\nu - B'_\nu) - (C''_\nu - B''_\nu)]K^2 \qquad \ldots (34)$$

where the + sign refers to the transition for which $\Delta K = +1$ and the - sign refers to $\Delta K = -1$. The P, Q and R branches of the sub-bands are then arranged the same way as in the parallel bands. The intensities of the lines in the perpendicular bands will be given by equation (31) where the intensity factor A_{JK} is given by:

$$\begin{aligned} \Delta J = +1 \qquad & A_{JK} = \frac{(J+2\pm K)(J+1\pm K)}{(J+1)(2J+1)} \\ \Delta J = 0 \qquad & A_{JK} = \frac{(J+1\pm K)(J\mp K)}{J(J+1)} \qquad \ldots (35) \\ \Delta J = -1 \qquad & A_{JK} = \frac{(J-1\mp K)(J\mp K)}{J(2J+1)} \end{aligned}$$

Equation (33) was given as $\Delta\nu = \frac{S(\beta)}{\pi}\sqrt{\frac{kT}{I_B}}$ in reference (9). The right side must be multiplied by the factor 1/c to make it dimensionally correct and numerically reasonable.

where the upper sign refers to $\Delta K = +1$, the lower sign refers to $\Delta K = -1$, and J and K refer to the initial state. The values for the $K = 0$ sub-band must be multiplied by two. Figure 4 shows a perpendicular band of CHF_3 calculated with the aid of these formulae. The value of ζ_i in equation (34) was taken to be zero for convenience. This constant different from zero would tend to increase or decrease the spread of the origins of the sub-bands depending on whether ζ_i was positive or negative. If the constant $\zeta_i \simeq -0.8$, then the factor $[C_\nu^\nu(1-\zeta_i) - B_\nu^\nu]$ in equation (34) would be approximately zero and the origins of the sub-bands would not vary with K. In such a case, the appearance of a perpendicular band would be approximately the same as that of a parallel band.

Transitions between two degenerate (E) levels will give rise to both parallel and perpendicular bands according to the species rules given in equation (18). The two bands will in general have very different magnitudes so that only one of the two components will contribute to the appearance of the absorption band.

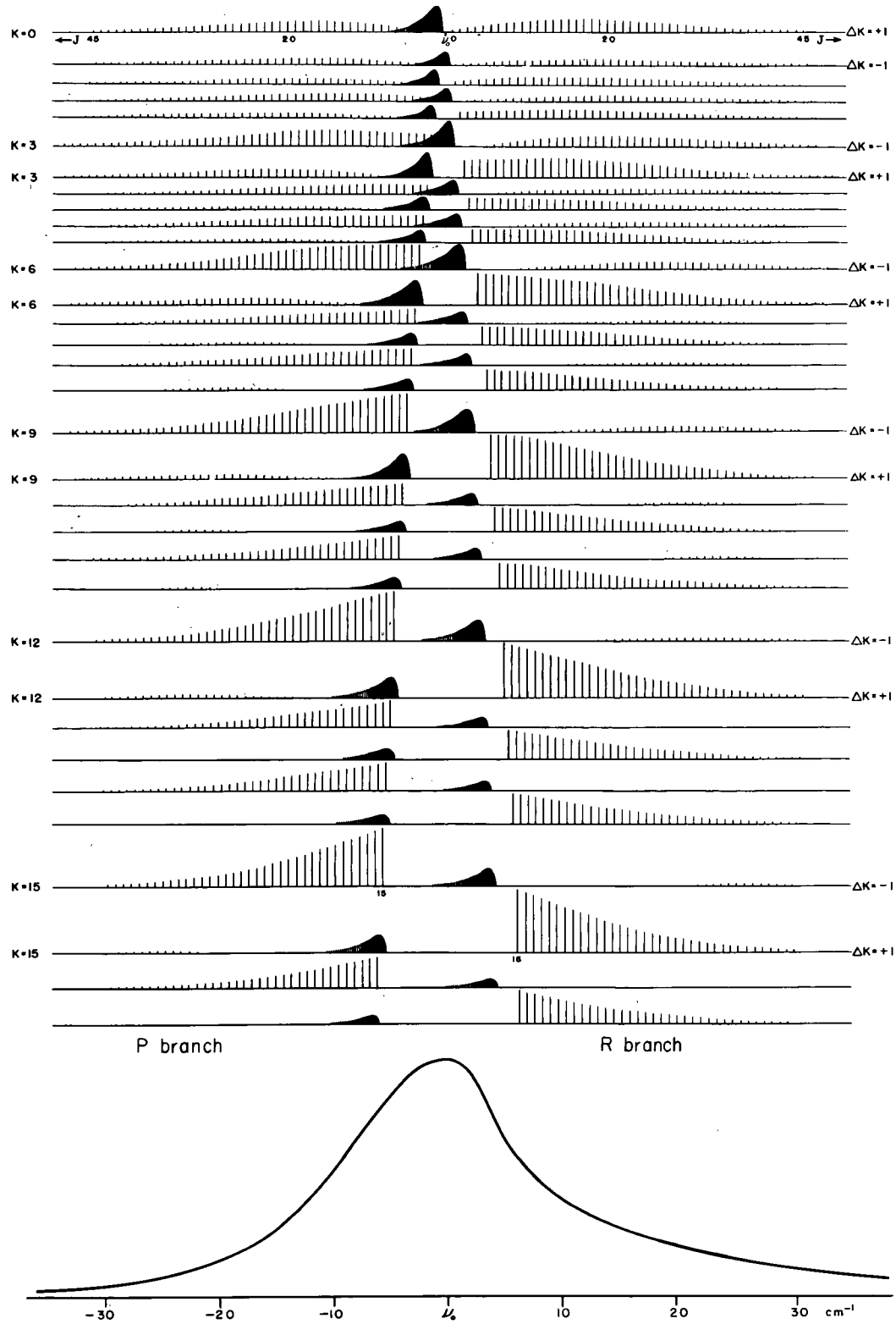

FIGURE 4. SUB-BANDS AND COMPLETE PERPENDICULAR BAND OF CHF_3. The peaks of the P and R branches increase up to K=23 and then decrease. Calculations are for a temperature of 300°K and $\zeta_i = 0$.

III EXPERIMENTAL PROCEDURE

1. Apparatus

a. The Spectrograph

The infrared spectrograph used was a Perkin-Elmer model 12-B with LiF, KBr and NaCl prisms, and a d.c. thermocouple detector. This particular instrument has been more fully described by Ross[10] and Little[11]. The sample cells used were a 10 cm. cell, a standard Perkin-Elmer meter cell, and a multiple path absorption cell described in section b.

b. The Multiple Path Absorption Cell.

In order to measure weak absorption bands, a long path length is necessary if the pressure is to be kept low enough to prevent pressure broadening and pressure shifts of some of the bands. The most practicable way of getting a long absorption path without having extremely large sample cells is by means of a multiple path absorption cell as first conceived by White[12]. The optical arrangement of the cell, shown in Figure 5, is the only type now used which will allow a large effective aperture.

It can be seen from Figure 5 that none of the light is lost by successive traversals. The light from the entrance slit is imaged by mirror A on point 1 of mirror C. Mirror C then images mirror A on mirror B and so on until the entrance slit is finally imaged on the exit slit. Due to the large number of off-axis reflections of the beam, it was suspected that the astigmatism of the final image

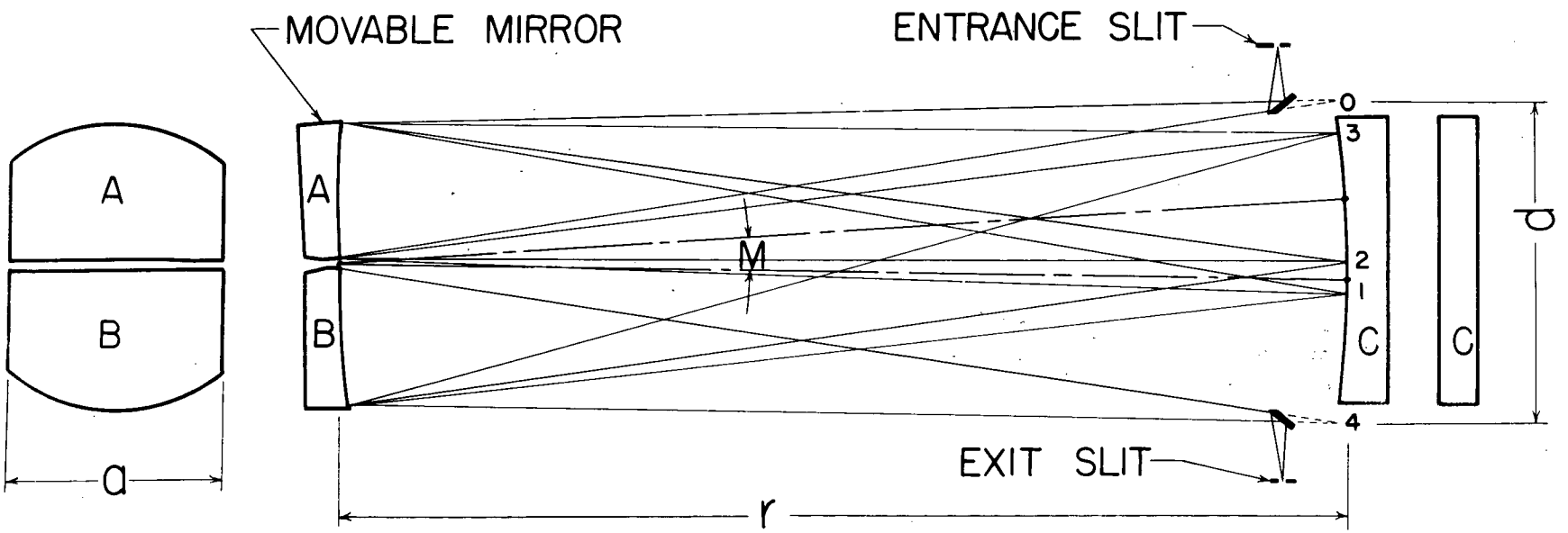

FIGURE 5. OPTICAL ARRANGEMENT OF ABSORPTION CELL SET FOR 8 TRAVERSALS.

would be so large that the intensity would be reduced. Calculations[13] showed however, that if the entrance slit of the cell were made longer than the entrance slit of the spectrometer, there would be no loss in intensity due to astigmatism. This calculation is given in the appendix.

The entire optical system of the cell is mounted on an aluminum channel and placed inside an eight inch diameter pipe with NaCl windows for entrance and exit beams. Figure 6 shows the instrument with the optical part taken outside the tank. All the mirrors have the necessary adjusting screws for horizontal and angular adjustment so that the mirrors can be adjusted while free of the tank and then placed inside. The channel rests on a three point suspension inside the tank so that any distortion of the tank due to evacuation will not affect the focus of the beam. The number of traversals of the beam is changed by turning a micrometer screw mounted on the outside of the tank. This rotates mirror A by means of a connecting shaft which passes through the side of the tank. A vacuum seal is maintained by mounting an "O" ring on the movable shaft so that the gas sample need not be disturbed when the number of traversals is changed. This feature has been found to be very convenient in practice.

One eight-inch diameter pyrex mirror was polished and cut as shown in Figure 7. This method of cutting ensures a cheaper and more efficient use of the mirror surfaces than by polishing two separate mirrors. The pyrex surfaces were coated with aluminum and magnesium

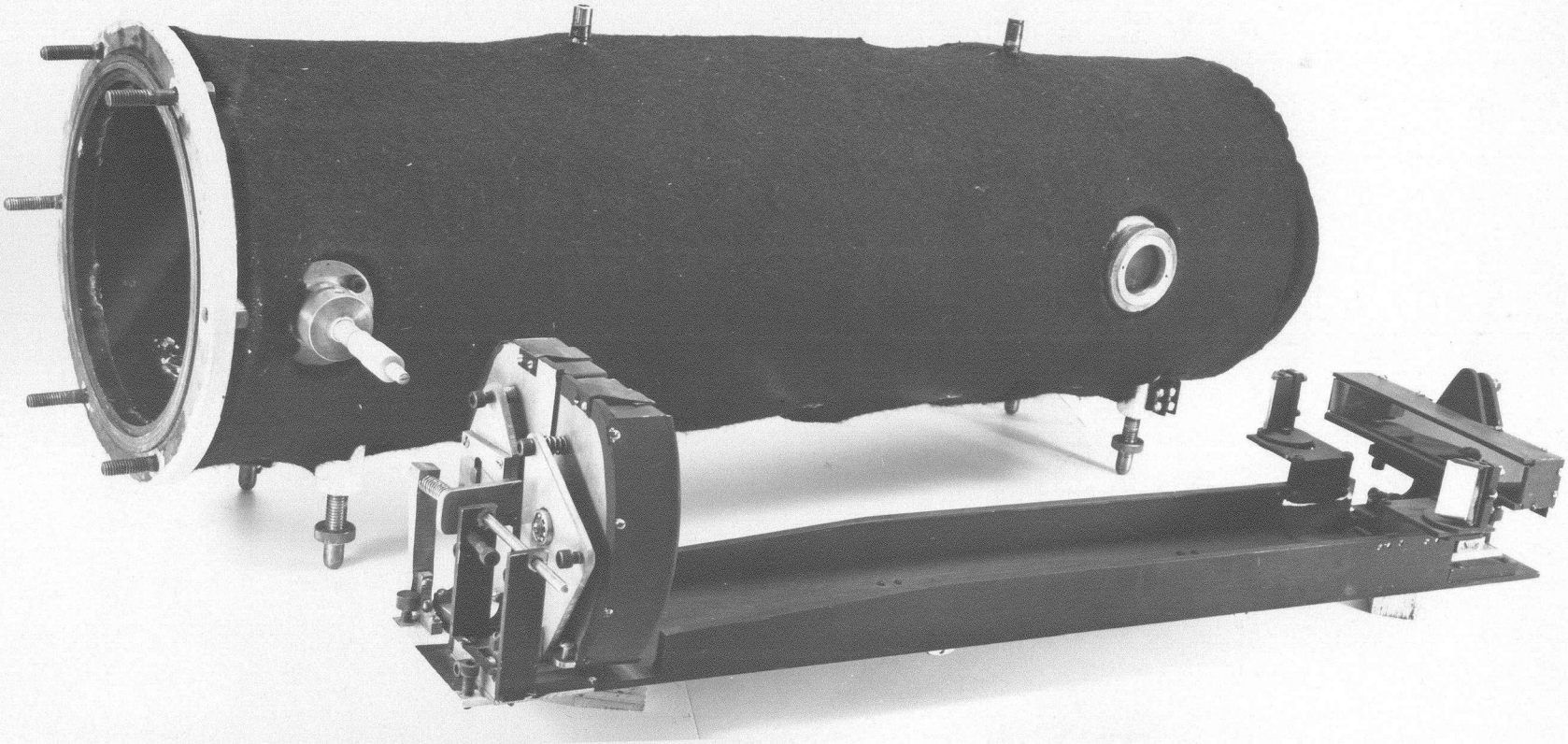

FIGURE 6. THE MULTIPLE PATH ABSORPTION CELL.

fluoride which gave a measured reflection coefficient of 0.96 in the near infrared.

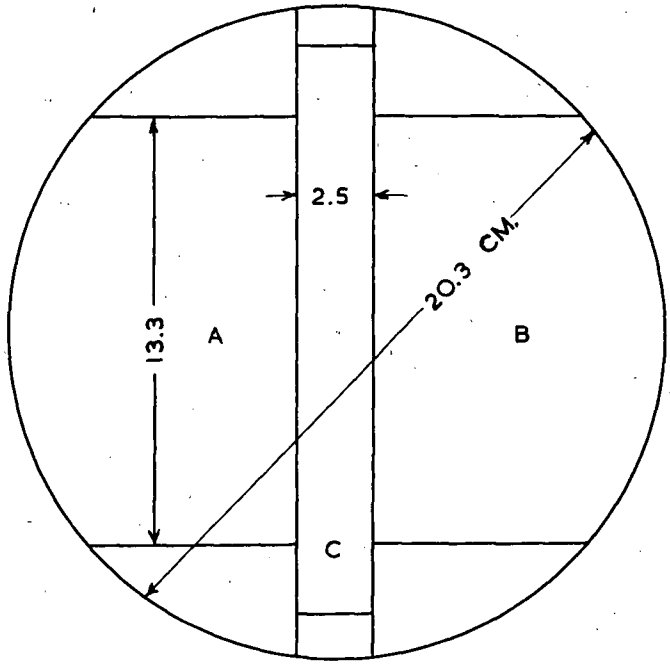

Figure 7. Cell Mirrors cut for most Efficient Use.

c. Sources

A globar was used with the 10 cm and meter cells but a brighter source was desirable for the multiple path cell because of the lower aperture of the allowed beam when this cell was used (f/6 compared to f/4.5 of the spectrograph). A large 2.5 mm diameter Nernst glower was used with this cell. This source was more stable than either the carbon arc or the smaller 1.3 mm diameter glower. The glower was placed in the position of the entrance slit, so that no mechanical entrance or exit slits were needed as the dimensions of the glower were of the proper size to act as an entrance slit.

2. Calibration

The method of calibration was that developed by Ross and Little[14]. The calibration points were fitted to the formula

$$\nu^2 = \nu_0^2 + \frac{a}{T - T_0} \qquad \ldots (36)$$

where T is the wave drive reading and the calculated constants ν_0^2, a and T_0 have no real significance. Above 4000 cm^{-1}, formula (36) does not fit over a large enough region to be useful so a calibration curve was drawn in this region.

The chief obstacle in the calibration was in the choosing of suitable calibration points. In most regions, the accuracy of the measurements was limited by the calibration points themselves. It would be desirable to have accurate calibration points listed to 0.1 cm^{-1} instead of to the nearest wave number as is given in the Perkin-Elmer calibration data.

The KBr region was calibrated using the water vapour data of Randall, Dennison, Ginsburg and Weber[15], the CO_2 data of Martin and Barker[16], and the 1-2-4 trichlorobenzene and polystyrene points of Plyler and Peters[17]. Although the grating spectra of water vapour had a much higher dispersion than could be obtained from the Perkin-Elmer spectrograph, the points could easily be correlated. This calibration for KBr was found to be far better than the calibration given in the Perkin-Elmer manual[18].

The calibration points used in all regions are listed in Table II. In addition to these, some of the points supplied by Plyler and Peters[17] were used in all three regions. The main objection to these calibration points (17) is that they are not spaced closely enough and some of the lines are broad.

Table II Calibration Points

LiF Region	NaCl Region
Hg Arc[17] 1-2-4-Trichlorobenzene[17] H_2O[19] NH_3, CH_4, HBr, CO_2, CO, H_2O } 18	H_2O, NH_3, CO_2 } 18
	KBr Region
	H_2O[15] 1-2-4 Trichlorobenzene[17] Polystyrene[17] CO_2[16]

IV RESULTS

In the region from 400 to 5540 cm^{-1}, over forty absorption bands were found. These bands with their assignments and calculated values are listed in Table III. All of the bands above 1700 cm^{-1} with intensities marked as very very weak (v.v.w.), were found by using the multiple path absorption cell.

Before discussing the analysis of the results, it is profitable to examine the appearance of the theoretical parallel and perpendicular bands shown in Figure 3 and Figure 4. First the appearance of the parallel band: It should be noted that the separation of the maxima of the P and R branches is 37 cm^{-1} and the dip on the high frequency side of the central Q branch is deeper than on the low frequency side. Also, the intensity of the R branch is slightly greater than that of the P branch. Figure 8(b) shows a band with these definite characteristics. The perpendicular band has less distinguishing characteristics. Under low resolution, it would show up as a single line with no characteristic structure or at best as a slightly non-symmetrical band, as shown in the theoretical trace of Figure 4 and also in the 1153 cm^{-1} line in Figure 8(a), with the steeper slope on the high frequency side. The perpendicular band may have an altogether different appearance depending on the value of the constant ζ_i^c as was pointed out in Section II-3-b.

Table III Infrared Absorption Bands of CHF_3

Observed cm^{-1}		Assignment#			Calculated
507.5	m.		ν_6	E	----
700.1	m.	//	ν_3	A	----
869	v.v.w.		$\nu_4 - \nu_6$	A + E	867.5
1015	v.w.		$2\nu_6$	A + E	1015
1153	v.s.	⊥	ν_5	E	----
1209	m.		$\nu_3 + \nu_6$	E	1208
1375	s.		ν_4	E	----
1658	w.		$\nu_5 + \nu_6$	A + E	1661
1716	v.v.w.		$2\nu_6 + \nu_3$	A + E	1715
1818	v.v.w.		$\nu_2 + \nu_3$	A	1817
1849	w.	⊥	$\nu_5 + \nu_3$	E	1853
1909	v.w.		$\nu_6 + 2\nu_3$	E	1908
2029	v.v.w.		$4\nu_6$	A + 2E	2030
2076 (double)	w.	⊥	$\nu_3 + \nu_4$	E	2075
2161 (d)	v.w.		$\nu_5 + 2\nu_6$	A + 2E	2168
2281	s.		$\nu_2 + \nu_5$	E	2270
2292 2303 2315	s. on CO_2		$2\nu_5$	A + E	2306
2408 2415	v.w.		$2\nu_3 + 2\nu_6$	A + E	2415
2517	v.s.		$\nu_4 + \nu_5$	A + E	2528

The species given is the species of $\psi_{\nu}^{U}\ \psi_{\nu}^{L}$ which is obtained by the multiplication rules (18). In all cases except for the difference bands, it is the species of the upper state.

Table III - Continued

Observed cm^{-1}		Assignment		Calculated
2692, 2709, 2728	s.	$2\nu_2 + \nu_6$	E	2742
2754	m.	$2\nu_4$	A + E	2750
2778	m.	$\nu_4 + 2\nu_3$	E	2775
3033	v.s.	// ν_1	A	———
3041	w.	$\nu_4 + \nu_5 + \nu_6$	A + 3E	3036
3183	v.w.	$\nu_2 + \nu_3 + \nu_4$	E	3192
3207	v.v.w.	$\nu_3 + \nu_4 + \nu_5$	A + E	3228
3255	v.v.w.	$2\nu_4 + \nu_6$	A + 3E	3258
3406	w.	$\nu_2 + 2\nu_5$	A + E	3423
3438	w.	$2\nu_4 + \nu_3$	A + E	3450
3483	v.v.w.	$3\nu_3 + \nu_4$	E	3475
3545	v.v.w.	$\nu_1 + \nu_6$	E	3541
3645 on H_2O bands	w.	$\nu_2 + \nu_4 + \nu_5$	A + E	3645
3740 on H_2O bands	w.	$\nu_1 + \nu_3$	A	3733
3850 on H_2O bands	w.	$\nu_2 + 2\nu_4$	A + E	3867
4045, 4056	v.v.w.	$\nu_1 + 2\nu_6$	A + E	4048
4171, 4186	s.	$\nu_1 + \nu_5$	E	4186
4210	v.w.	$\nu_1 + \nu_3 + \nu_6$	E	4241
4342	v.v.w.	$\nu_1 + \nu_3 + \nu_4 + \nu_5$	A + E	4345
4405 (d)	s.	$\nu_1 + \nu_4$	E	4408
4515	v.v.w.	$3\nu_2 + \nu_5$	E	4504

Table III - Continued

Observed cm^{-1}		Assignment		Calculated
4550	v.v.w.	$\nu_1 + 3\nu_6$	A + E	4556
4691	v.v.w.	$\nu_1 + \nu_5 + \nu_6$	A + E	4694
4716	v.v.w.	$\nu_1 + \nu_3 + 2\nu_6$	A + E	4748
4770	v.v.w.	$2\nu_2 + \nu_4 + \nu_5$	A + E	4762
4877	v.v.w.	$\nu_1 + \nu_3 + \nu_5$	E	4886
4987	v.v.w.	$\nu_1 + \nu_3 + \nu_4$	E	5108
5185	w.	$\nu_1 + \nu_5 + 2\nu_6$	A + 2E	5201
5340	w.	$\nu_1 + 2\nu_5$	A + E	5339
5541	w.	$\nu_1 + \nu_4 + \nu_5$	A + E	5561

The band at 700.1 cm^{-1} has the appearance of the parallel band shown in Figure 3. This is contrary to the statement by Price[1] that the 700.1 cm^{-1} band had an indifferent appearance. The 507.5 cm^{-1} band also has the appearance of a parallel band but in view of the depolarization measurements of Rank, Schull and Pace[5], it is considered to be a perpendicular band with the coriolis constant $\zeta_6 \simeq -0.8$. This assignment is consistant with the bands $\nu_4 - \nu_6$, $\nu_3 + \nu_6$, $2\nu_2 + \nu_6$ and $2\nu_3 + \nu_6$ all of which are perpendicular bands but have the appearance of parallel bands.

The bands 2709, 2754 and 2778 cm^{-1} are difficult to assign. There is probably some displacement of all three due to Fermi resonance, and in addition, the 2778 cm^{-1} band could equally well be $\nu_2 + \nu_5 + \nu_6$ or $\nu_4 + 2\nu_3$ because the

interaction constants are not well enough known to help decide between them. The group of bands 3183, 3207 and 3255 cm^{-1} shown in Figure 8(d) is also difficult to assign because of Fermi resonance and overlapping structures.

The 3033 cm^{-1} band shown in Figure 8(c) was identified as a parallel band with the R branch peak at +20 cm^{-1} and the P branch peak at -17 cm^{-1} from the band centre. This assignment is most probable because this frequency is characteristic of the ≡C-H stretching vibration in other molecules and would give rise to a strong parallel band. The extra line between the Q and R branches at 3041 cm^{-1} is considered to be due to an entirely different transition.

The only overtone series found was ν_6, $2\nu_6$ and $4\nu_6$. The line $3\nu_6$ would be difficult to find because it would lie on the H_2O rotation bands which are always present in the spectrogram. The anharmonicity term χ_{66} would then be $\chi_{66} = -0.08$ cm^{-1} according to equation (21).

The assignment of bands with higher wave numbers becomes increasingly difficult because the resolution is usually not high enough to give any observable structure that might help in the assignment. Also the anharmonicity terms are not known well enough to calculate more closely the expected band frequency. An attempt was made to calculate all the anharmonicity constants but it was found that there were too many inconsistencies with the data available. Only 14 of the 21 double combination bands, which would

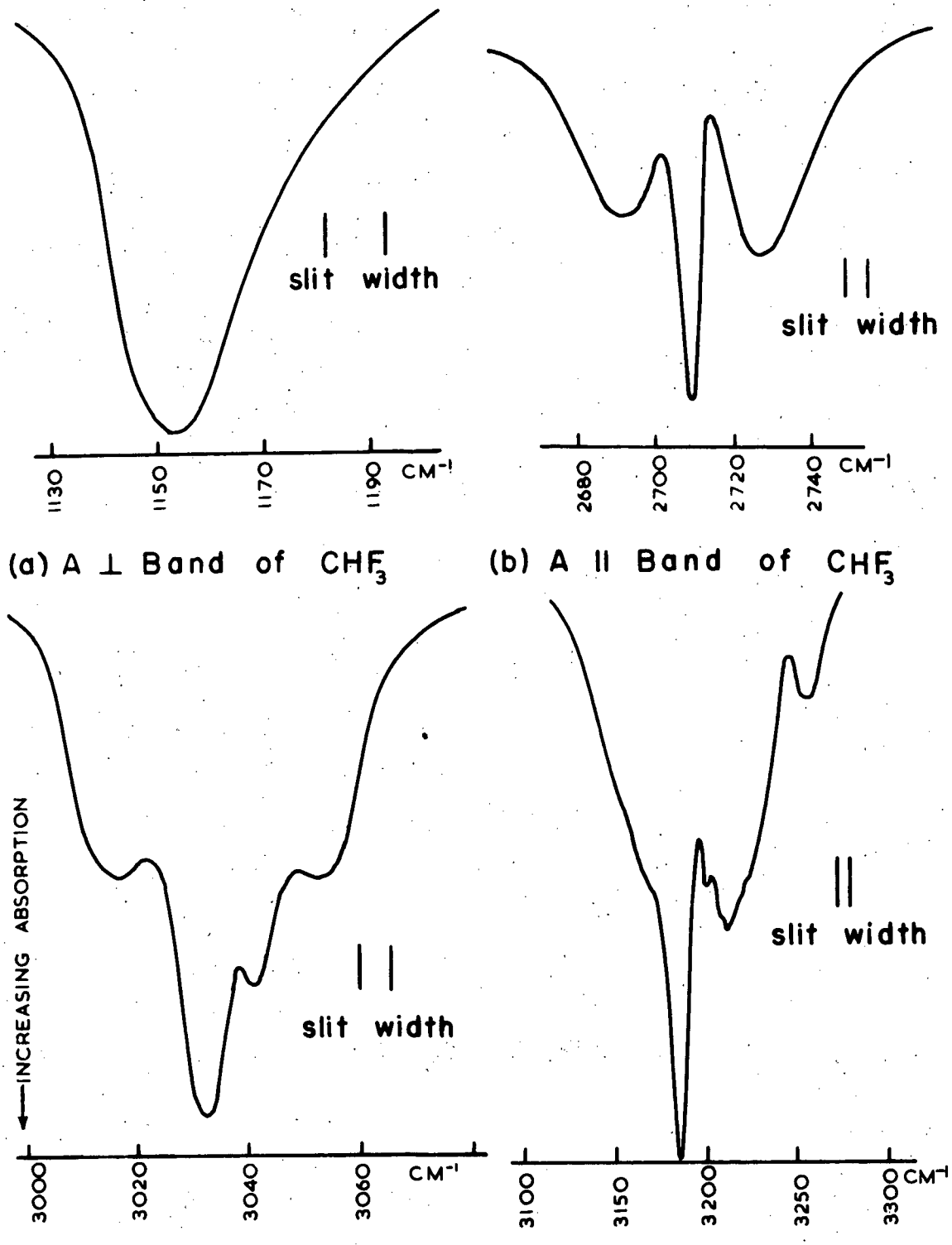

FIGURE 8. ABSORPTION BANDS OF CHF_3

give the anharmonicity constants directly, were found. Even some of these may have been affected by Fermi resonance.

It was hoped that one of the difference bands $\nu_2 - \nu_6$, $\nu_2 - \nu_3$, or even $\nu_1 - \nu_2$ could be found to establish a more direct measurement for ν_2 than the Raman value of 1117 cm^{-1} for liquid fluoroform. As none of these bands were found, the value of 1117 cm^{-1} was used for ν_2 in all assignments. Altogether, ν_2 was assigned in seven combination bands, the most certain of which was the 1818 cm^{-1} band.

V CONCLUSION

The assignment of the fundamental vibrations by Rank, Schull and Pace[5] has been found consistent with the observed spectrum. The apparent discrepancy in the appearance of ν_6 as a parallel band has been explained and the anharmonicity constant x_{66} was calculated to be -0.08 cm^{-1}. The other anharmonicity and interaction constants were sufficiently uncertain as to require an examination under higher dispersion to calculate them with any degree of certainty. The fundamental vibration lines were remeasured to be:

ν_1 3033 cm^{-1}

ν_2 (1117)[5]

ν_3 700.1

ν_4 1375

ν_5 1153

ν_6 507.5

APPENDIX

The Astigmatism of a Multiple Path Absorption Cell

The number of traversals, N, of the light beam through the length of the cell is given by $N = 2d/Mr$ where d, M and r are shown in Figure 5. The astigmatism can be calculated as follows: For the vertical line image,

$\frac{1}{S} + \frac{1}{S_1} = \frac{2}{r \cos\phi}$ where S_1 = vertical line image distance,

S = object distance $\simeq$ radius of curvature, r, and

ϕ = off-axis angle. For the horizontal line image,

$\frac{1}{S} + \frac{1}{S_2} = \frac{2\cos\phi}{r}$ where S_2 = horizontal line image distance,

$$\Delta\left(\frac{1}{S}\right) = \frac{1}{S_1} - \frac{1}{S_2} = \frac{2}{r\cos\phi} - \frac{2\cos\phi}{r} \simeq \frac{\Delta S}{S^2}$$

where ΔS = distance between horizontal and vertical line images.

$$\Delta S \simeq \frac{2r}{\cos\phi} - 2r\cos\phi \simeq 2r\left[\left(1+\frac{\phi^2}{2!}+5\frac{\phi^4}{4!}+\cdots\right)-\left(1-\frac{\phi^2}{2!}+\frac{\phi^4}{4!}-\cdots\right)\right] \simeq +2r\phi^2$$

The astigmatism is additive on each reflection since

$\frac{1}{p} + \frac{1}{q} = \frac{2}{r}$ ... simple mirror formula

$\frac{\Delta p}{p^2} + \frac{\Delta q}{q^2} \simeq 0$

$\Delta p \simeq -\left(\frac{p}{q}\right)^2(\Delta q) \simeq -(\Delta q)$ since $p \simeq q \simeq r$

Therefore the astigmatism is additive if the distance between the horizontal and vertical line images is small compared to r. Therefore $\Delta S \simeq 2r(\phi_1^2 + \phi_2^2 + \cdots + \phi_{N/2}^2)$

where the ϕ_i are the successive off-axis angles.

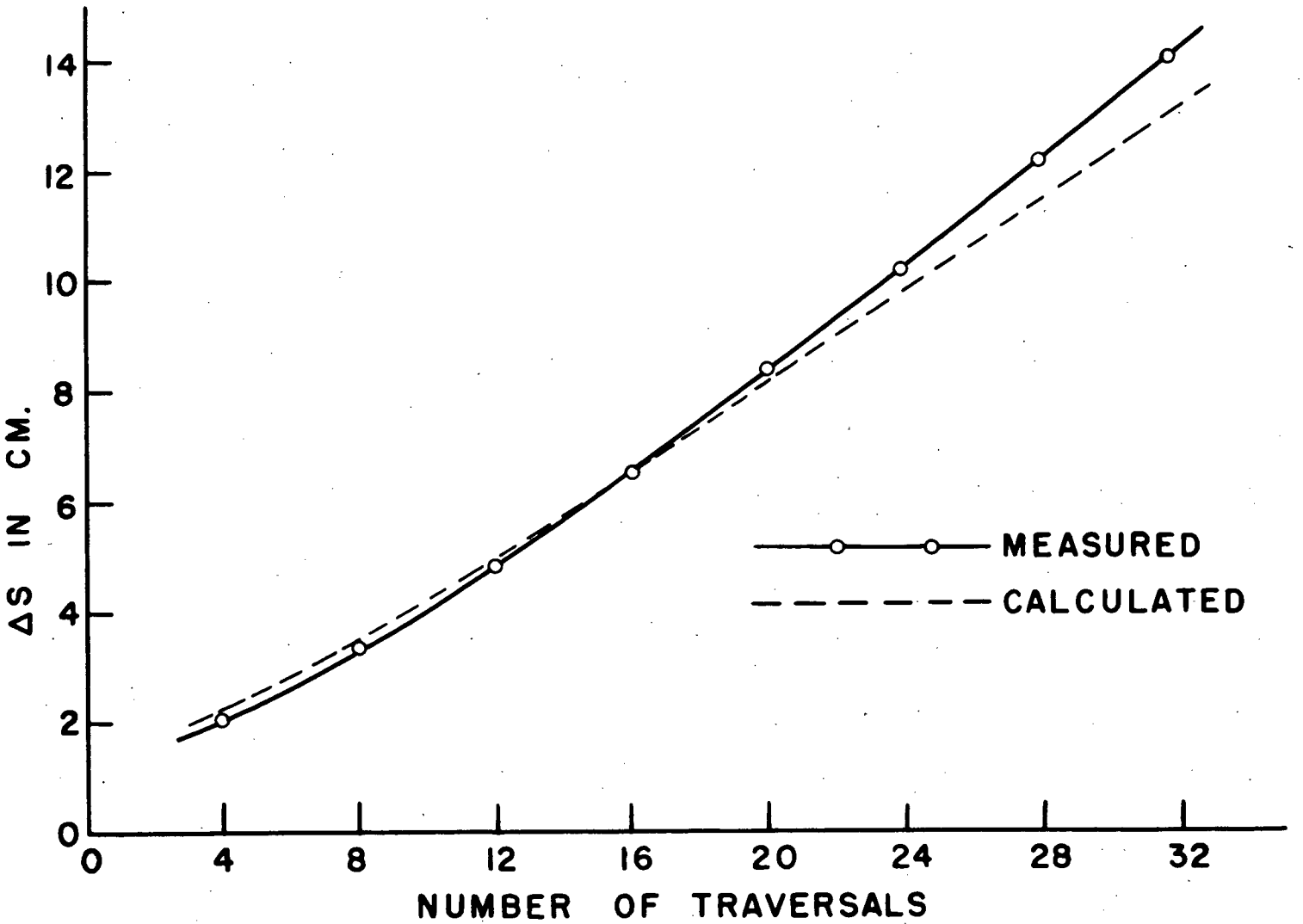

FIGURE 9. ASTIGMATISM OF ABSORPTION CELL.

By calculating the successive angles ϕ_i, it is easy to show that

$$\sum_{i=1}^{N/2} \phi_i^2 = [1+2^2+3^2+\cdots+(\tfrac{N}{2})^2]M^2 - 2(1+2+\cdots+\tfrac{N}{2})M\theta + \tfrac{N}{2}\theta^2$$

where θ = angle between source and axis of fixed mirror. Using M = 2d/rN and θ = d/2r (may be slightly greater depending on the geometrical set up), the formula can be further simplified to $\Delta S = \frac{2d^2}{r}\left[\frac{4}{N}\sum_{i=1}^{N/2} i^2 - \frac{N}{8} - \frac{1}{2}\right]$

The measured and calculated values of astigmatism up to 32 traversals are shown in Figure 9. In low aperture instruments the agreement would be even better than that shown.

One would expect some loss in intensity of the exit beam due to the astigmatism. By using simple geometry, however, it can be seen that if the instrument is adjusted to be in focus for the vertical line image, and the entrance slit is made longer than the exit slit by an amount $\frac{\Delta s\, q}{r}$, then there will be no loss in intensity due to astigmatism.

Bibliography

1. W. C. Price, unpublished, reported by Bernstein and Herzberg[2].

2. H. J. Bernstein and G. Herzberg, J. Chem. Phys.,16,30,1948.

3. G. Glocker and G. R. Leader, J. Chem. Phys., 8, 699, 1940.

4. G. Glocker and W. F. Edgell, J. Chem. Phys. 9, 224, 1941.

5. D. H. Rank, E. R. Schull and E. L. Pace, J. Chem. Phys., 18, 885, 1950.

6. O. R. Gillam, H. D. Edwards and Walter Gordy, Phys. Rev., 75, 1014, 1949.

7. G. Herzberg, Molecular Spectra and Molecular Structure, II Infrared and Raman Spectra of Polyatomic Molecules. (D. Van Nostrand, New York, 1945).

8. L. Pauling and E. B. Wilson Jr., Introduction to Quantum Mechanics. (McGraw Hill, New York, 1935).

9. S. L. Gerhard and D. M. Dennison, Phys. Rev., 43,197,1933.

10. W. L. Ross, Thesis for the degree of Master of Arts, U. B. C., 1950.

11. D. E. Little, Thesis for the degree of Master of Arts, U. B. C., 1950.

12. J. U. White, J. O. S. A., 32, 285, 1942.

13. E. R. Reesor, J. O. S. A., 41, 1059, 1951.

14. W. L. Ross and D. E. Little, J. O. S. A., 41,1006, 1951.

15. H. M. Randall, D. M. Dennison, N. G. Ginsburg and L. R. Weber, Phys. Rev., 52, 160, 1937.

16. P. E. Martin and E. F. Barker, Phys. Rev., 41, 291, 1932.

17. E. K. Plyler and C. W. Peters, J. Res. Nat. Bur. Std., 45, 462, 1950.

18. Perkin-Elmer Corporation, Instruction Manual, Model 12-C

19. W. W. Sleator, Astrophys. J., 48, 125, 1918.